

An integrated modular approach to modeling sand production and cavity growth with emphasis on the multiphase flow and 3D effects

J. Wang¹, D. Walters², A. Settari³, R. G. Wan⁴

^{1,2}*Taurus Reservoir Solutions Ltd.*, ³*Department of Chemical and Petroleum Engineering, University of Calgary*, ⁴*Department of Civil Engineering, University of Calgary*

Copyright 2006, ARMA, American Rock Mechanics Association

This paper was prepared for presentation at Golden Rocks 2006, The 41st U.S. Symposium on Rock Mechanics (USRMS): "50 Years of Rock Mechanics - Landmarks and Future Challenges", held in Golden, Colorado, June 17-21, 2006.

This paper was selected for presentation by a USRMS Program Committee following review of information contained in an abstract submitted earlier by the author(s). Contents of the paper, as presented, have not been reviewed by ARMA/USRMS and are subject to correction by the author(s). The material, as presented, does not necessarily reflect any position of USRMS, ARMA, their officers, or members. Electronic reproduction, distribution, or storage of any part of this paper for commercial purposes without the written consent of ARMA is prohibited. Permission to reproduce in print is restricted to an abstract of not more than 300 words; illustrations may not be copied. The abstract must contain conspicuous acknowledgement of where and by whom the paper was presented.

ABSTRACT: This paper extends earlier work on sand production modeling in any type of light and heavy oil reservoirs within an unconsolidated and/or weakly consolidated formation. A fully coupled reservoir-erosion-geomechanics model is presented to predict volumetric sand production and cavity growth under 3-D, multiphase flow conditions. This model is based on mixture theory with erosion mechanics, in which multiphase hydrodynamics and geomechanics are coupled in a consistent manner via principal unknowns, such as saturation, pressure, porosity, and formation displacements. An integrated modular approach is adopted to effectively take advantage of the current advanced standard reservoir and stress-strain codes, and is implemented into three integrated computational modules, i.e. erosion module, reservoir module, and geomechanics module. The system is powerful in terms of its capabilities, yet practical in terms of computer requirements. Numerical results on field studies are presented to illustrate the new capabilities of the model. The effects of multiphase flow (water-cut) and 3D geometry are particularly examined to demonstrate the impact on the volumetric sand production and cavity growth.

1. INTRODUCTION

The production of sand is a long-standing problem from unconsolidated and/or weakly consolidated formations during the hydrocarbon recovery. It has been studied extensively for years by many researchers and engineers. However, precisely addressing this problem remains unsolved due to its complexity. Sand production occurs from a well after the reservoir formation is either shear or tensile failed under the imposed stress changes during the hydrocarbon production. The oil or gas flow transports the failed fine sand particles to the surface facilities, while leaving the coarse ones in the wellbore. When the accumulated sand column is high enough to cover the perforations, the well is killed. This is called "sand-up". Sanding results in, but not limited to, reduction of life cycles of equipments, stability of a wellbore, and treatment of unwanted sand in an environmental acceptable manner. On the other hand, limited sand production has been proven to significantly increase the well productivity when tolerating it at a manageable level in both conventional light and heavy oil reservoirs [1]. Therefore, sand production and

control remain critical challenges in reservoir management and field operations.

It has been of particular interest to the oil operators to reliably estimate the amount and concentration of the produced sand. Over the past decade, considerable efforts have been made in developing robust methods for predicting the onset of sand production. The application would be utilized at the reservoir appraisal stage, where the risk of sand production must be quantified to evaluate the reservoir management strategy or to satisfy regulatory authorities. There are usually no historical sanding data, and the focus is on predicting the conditions under which sand production might occur. In recent years, attention has been focused on establishing methodologies for predicting the volumetric sand and its rate in fields where sand production has been encountered and must be economically managed or controlled. The goal is to regulate and control sand production rather than the often unwarranted and widespread adoption of costly sand exclusion/retention measures. Hence, it is imperative to find an efficient computational model that has the predictive capability to assist field operators to develop and

monitor the optimal sand management and control strategies. The ultimate goal is to design economical well-production schedules through which oil producers might not only design better pumping schemes for sand management, but also maximize productivity and ensure completion longevity.

The hydro-erosion model, first proposed by Vardoulakis et al. [2], is based on rigid porous media (no skeleton deformation) in which mass balance is applied to a three-constituent system comprised of solid, fluid and fluidized solid using homogenization mixture theory. Subsequently, Wan and Wang [3,4] extended this pure erosion model to include the effect of the deformation of porous media in a consistent manner. A single-phase flow is fully coupled with geomechanics within a continuum mechanics framework. Furthermore, Wang et al. [5,6] extended previous work to a fully coupled reservoir-geomechanics model to account for the effects of multiphase flow and geomechanics in a consistent manner. This approach results in solving a set of coupled non-linear time-dependent equations with fluidized solid concentration (saturation), fluid pressure, porosity, and deformation as main variables. The model has been proven to be a viable tool in terms of matching numerical calculations with lab test and field data [7]. As the hydrocarbon production takes place, the erosion process begins as a result of the degradation of the sand matrix strength and the drag force imposed by fluid pressure gradient. The plastic yielding zones develop over time due to the material degradation (erosion) and stress re-distribution, while the wormholes or cavities form and propagate in terms of the increasing porosity values at an intensive erosion range. The volumetric oil and sand productions are also calculated as a function of time, stresses, and hydrocarbon flow rate. An oilwell study subject to different completion schemes (perforated casing and open-hole completion) was presented using the coupled reservoir-geomechanical model [8]. The results of two types of completion (open-hole and perforated casing completion) give an insight to guide the design using different completion techniques and perforation patterns so as to optimize the hydrocarbon production.

In this paper, we will further investigate and validate this model, then emphasize on its field application, i.e. multiphase (water-cut) and three-dimensional effects in particular.

2. GOVERNING EQUATIONS FOR COUPLED MULTIPHASE FLOW AND GEOMECHANICS WITH EROSION MECHANICS

Followed by common approach in continuum mechanics, the porous media can be idealized as a Representative Elementary Volume (REV) which comprises of five phases, namely solid grains (*s*), fluidized solids (*fs*), fluid (*f*), water (*w*) and gas (*g*) as shown in Figure 1. In reality, the individual distribution varies discontinuously over space. However, an averaging procedure in the spirit of mixture theory is used to homogenize each constituent over the REV volume *V* such that these individuals are substituted with continuous ones that fill the whole volume. Each phase discontinuity in the REV is represented by its own volume fraction, i.e. saturation and porosity. For each phase, mass balance, equilibrium, and erosion mechanical equations can be derived. Full details of derivations can be found in Wang et al. [6]. The set of governing equations are summarized as following.

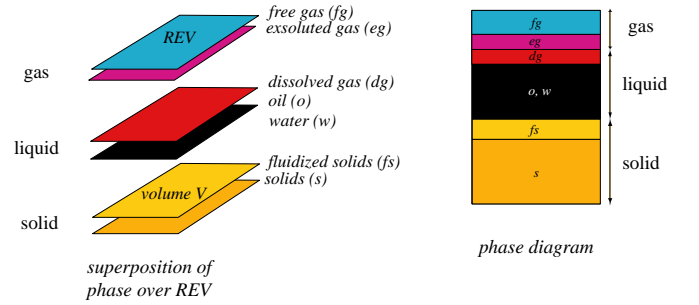


Fig. 1. Phase components of a REV.

- Generalized reservoir mass balance equations:

$$\nabla \cdot \left[\frac{\mathbf{v}_o}{B_o} + \frac{S_o \phi \dot{\mathbf{u}}_s}{B_o} \right] + \frac{\partial}{\partial t} \left[\frac{\phi S_o}{B_o} \right] = 0. \quad (1)$$

$$\nabla \cdot \left[\frac{\mathbf{v}_g}{B_g} + \frac{S_g \phi \dot{\mathbf{u}}_s}{B_g} + \frac{R_s \mathbf{v}_o}{B_o} + \frac{R_s S_o \phi \dot{\mathbf{u}}_s}{B_o} \right] + \frac{\partial}{\partial t} \left[\frac{\phi R_s S_o}{B_o} + \frac{\phi S_g}{B_g} \right] = 0. \quad (2)$$

$$\nabla \cdot \left[\frac{\mathbf{v}_w}{B_w} + \frac{S_w \phi \dot{\mathbf{u}}_s}{B_w} \right] + \frac{\partial}{\partial t} \left[\frac{\phi S_w}{B_w} \right] = 0. \quad (3)$$

where ϕ = porosity, S_i = saturations, B_i = the formation volume factors, ρ_i = the densities at stock tank

condition, \mathbf{v}_i = volumetric velocity of each phase ($i=o, g, w, fs$), R_s = the solution gas oil ratio, $\dot{\mathbf{u}}_s$ = the volume-weighted velocity of deforming solid skeleton.

- Erosion mechanical equations:

$$-\frac{\partial \phi}{\partial t} + \nabla \cdot [(1-\phi)\dot{\mathbf{u}}_s] + \frac{\dot{m}}{\rho_s} = 0. \quad (4)$$

$$\frac{\partial [\phi(S_{fs}-1)]}{\partial t} + \nabla \cdot [S_{fs}\mathbf{v}_m + (1-\phi+S_{fs})\dot{\mathbf{u}}_s] = 0. \quad (5)$$

where $\frac{\dot{m}}{\rho_s}$ = the source or sink term to account for the local rate of solid loss or gain per unit volume due to erosion.

- Equilibrium equations:

$$\nabla \cdot (\boldsymbol{\sigma}^{eff} - \omega P_m \mathbf{1}) + \mathbf{b} = \mathbf{0}. \quad (6)$$

where $\boldsymbol{\sigma}^{eff}$ = effective stress, \mathbf{b} are body forces per unit volume, and ω is Biot coefficient accounting for the compressibility of the sand grains. $\mathbf{1}$ is the Kronecker delta tensor such that $\mathbf{1}_{ij} = \delta_{ij}$. The averaged mixture pressure can be defined as $P_m = S_o P_o + S_g P_g + S_w P_w$.

- Constitutive laws:

Before above governing equations can be solved, constitutive laws describing sand particle erosion, fluid flow, and deformation of the sand matrix must be supplemented. It is commonly believed that the driving force causing the solid detachment from the sand matrix is due to hydrodynamics and geomechanics. Based on phenomenology, a possible functional form of mass generation can be extended from the inverse of filtration theory as proposed in refs. [2,9].

$$\frac{\dot{m}}{\rho_s} = \lambda(1-\phi)S_{fs} \left(1 - \frac{S_{fs}}{S_{fsc}}\right) \|\mathbf{v}_m\| \quad \text{if } \|\mathbf{v}_m\| \geq \|\mathbf{v}_m^{cr}\| \quad (7)$$

$$= 0 \quad \text{if } \|\mathbf{v}_m\| < \|\mathbf{v}_m^{cr}\|$$

where \mathbf{v}_m^{cr} is the critical average velocity of mixture below which no sand production occurs. The critical sand saturation Scr prevents all the mass eroded away. As sand saturation increases, more sand can

be deposited. Therefore, erosion and deposition balance each other when sand saturation reach the critical value. The erosion coefficient λ provides a length scale that can be linked to the accumulated plastic strains γ^p through the following relationship, i.e.

$$\lambda = \lambda(\gamma^p) = \lambda_0 + \frac{\gamma^p / \gamma_{max}^p}{\alpha + \beta \gamma^p / \gamma_{max}^p} \quad (8)$$

where α and β are constants to be determined, while λ_0 is a constant, and γ_{max}^p corresponds to the maximum plastic shear strain calculated for the entire domain.

The average velocity of mixture is defined as

$$\mathbf{v}_m = w_o S_o \mathbf{v}_o + w_g S_g \mathbf{v}_g + w_w S_w \mathbf{v}_w \quad (9)$$

where w_j ($j=o, g, w$) is the weighting factors which can be determined from rock wetness. It can also be linked to capillary force or phase saturation.

As for describing fluid flow, Darcy's law or non-Darcy's law is used to establish the relation between pressure gradient ∇p_j and discharge velocity \mathbf{v}_j for phases and the mixture. The permeability tensor can be related to porosity via the variation of Carman-Kozeny equation or any lab-determined table based core analysis [6]. Turning to solid skeleton deformations, an elasto-plastic constitutive law incorporating dilatancy together with Drucker-Prager failure criterion is used to describe the behavior of the solid skeleton dominated by grain slippage, rearrangement, dilation and de-structuration under compression and shear [1].

3. NUMERICAL STRATEGY

Having the governing equations and constitutive laws ready, the solution seems to be straightforward. However, the numerical stability problem arises due to the nature of these sets of equation [10]. Over the past years, the authors developed a generic numerical stabilization scheme - *an optimized local mean technique*. By enriching main field variables with high gradient terms, sharp *non-local* changes can be captured in the computations to ensure stable solutions [5].

Ideally, the coupled equations should be solved simultaneously due to the characteristics of their strong nonlinearity. However, it requires intensive computational power in terms of solving multiple variables at the same time. Moreover, it needs large code development and difficulties of future maintenance.

3.1. Modular approach

Modular approach has been prevailed due to its high efficiency, easy implementation, and above all accuracy if iterated to full convergence. Hence, an integrated modular approach is adopted to incorporate this stress-flow-erosion model, of which current advanced standard reservoir and stress-strain codes are effectively taken advantage with minimum development efforts. More precisely, this model is reformulated into three integrated computational modules, i.e. erosion module, reservoir module, and geomechanics module. The communication of each module is fulfilled by the data passing among the interfaces of modules. Depending on the complexity of addressed problems, different coupling methods among modules can be used, i.e. decoupled, explicitly coupled, iteratively coupled [11,12].

Decoupled: The reservoir module of the coupled system acts like a driver, only supplies pressure, temperature, flux, etc.. It does not receive coupled terms back from the geomechanics and erosion modules. This is also called one way coupling. Decoupled method can give quick results, while the accuracy of the results is questionable.

Explicitly coupled: This can be achieved by lagging the coupling terms one time step behind. Based on the previous stress and erosion solution, the reservoir simulator calculates the compressibility coefficient, stress or porosity dependent flow properties, and seeks for the flow solution. Then the stress and erosion solution are advanced to current time using the pressure, temperature and flux based on the calculated flow solution. The method is especially useful if the time step is very small, yet the accuracy is high.

Iteratively coupled: The iterative method consists of the repeated solutions of the reservoir, erosion, and stress equations during the time step until certain convergence criteria are met. It is noted that the explicit coupling is a special case of the iteratively coupled system in which only one

iteration is performed per time step. It is worth to mention that the iteratively coupled method solves the problem as rigorously as a fully coupled (simultaneous) solution if iterated to full convergence.

Hence, the degree of coupling among reservoir, erosion and geomechanics can be modulated at will depending on the level of computations ranging from independent reservoir, erosion, and stress solutions to a fully coupled system. As we might notice, the data passing among modules are crucial for the success of this approach. The data passing among the modules is illustrated in Figure 2.

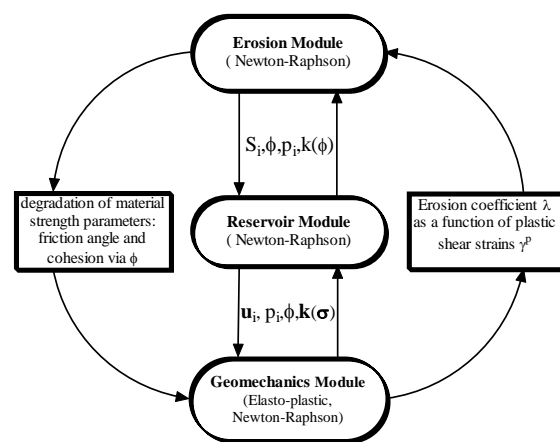


Fig. 2. Schematic of the coupled system architecture.

Coupling between reservoir and geomechanics: This can be done through pore volume changes and stress-dependent flow properties. Due to the flow pressure load, the geomechanics module calculates the volumetric changes, which can be related to porosity changes into the reservoir module. The pore volume change is an important recovery mechanism accounting for a large part of the production. Another effect is the stress dependence of permeability [11], as the stress redistribution might alter the reservoir permeability as a result of isotropic expansion/compression and/or the creations of shear planes.

Coupling between erosion and reservoir: Porosity increases due to enhanced permeability, as described by the variation of Carman-Kozeny equation or the table form from lab test. In return, erosion activity intensifies with an increase of flow flux as the pressure distribution is modified in reservoir module. As the viscosity is altered due to the content change in the mixture fluid, the reservoir viscosity profile is also modified by

fluidized sand saturation. The relationship can be determined from lab test.

Coupling between geomechanics and erosion:

Plastic shear deformations, incurred in the solid matrix under fluid and stress gradients, increase the solid erosion potential in Eq. (8). In return, the erosion process weakens the solid matrix through degradation of its mechanical strength, i.e. Young’s Modulus, friction angle, cohesion, etc.

3.2. Computational procedure - iterative coupling

The iterative coupling could be time-consuming and computationally ineffective to achieve the same accuracy as fully coupled solution [12]. Hence, the implementation of this modular approach needs a robust interface among modules, where the computer memory handling and data passing take place. The computational procedure is summarized as following.

- (a) The reservoir module is solved to give pore pressure, temperature, and velocity of each phase profile from reservoir module based on boundary conditions and initial values.
- (b) The geomechanics module is solved based on the pore pressure and temperature profile from (a) as load vectors. Sanding tendency (onset of sand production prediction) is determined by checking whether the formation is shear or tensile failed in this step.
- (c) Based on whether critical velocity exceeds in Eq. (7) and whether formation is failed in Eq. (8), erosion module is solved for two primary variables -- fluidized sand saturation and porosity.
- (d) With updated coupling terms from geomechanics module and updated permeability and viscosity from erosion module, reservoir module is re-solved.
- (e) Repeat (b) to (d) until certain convergence criteria are met. Then move to next time step.

It is worth to mention that Newton-Rhapson scheme is used to speed up calculations in each module calculation to ensure each module converges

quadratically with limited steps. It is also noted that the calculation on sand initiation and production is automatically embedded in the computational procedure. Individual module is triggered to solve for the primary variables upon certain criteria meet.

3.3. Validation against fully coupled solution

As stated before, iteratively coupling could give the wrong solution if the implementation is not handled properly. In this section, a single-phase one-dimensional problem will be used to validate the model. A segment of a fictional reservoir of length $L=1\text{ m}$ with an initial porosity $\phi_0=0.25$ and an initial fluidized sand concentration $c_0=0.0002$ is considered. The drawdown pressure between $x=0$ and $x=L$ is taken as 10 MPa, while the erosion parameter λ is 10m^{-1} . As far as fluid properties are concerned, a single-phase heavy oil with a viscosity and an initial formation permeability $k_{ox}=k_{oy}=15$ Darcy are considered. Time step $\Delta t=0.01$ day, and total simulation time = 2 days.

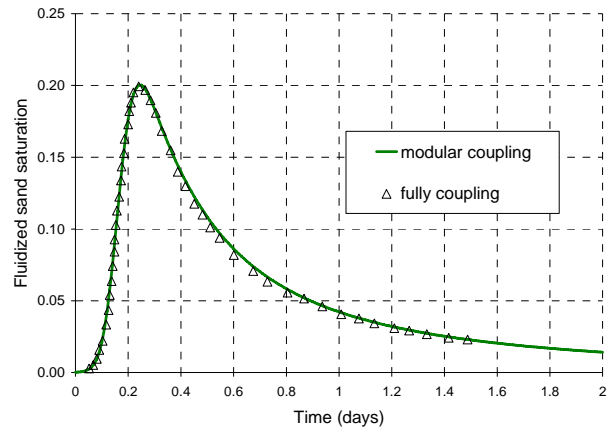


Fig. 3. Fluidized sand saturation history at wellbore.

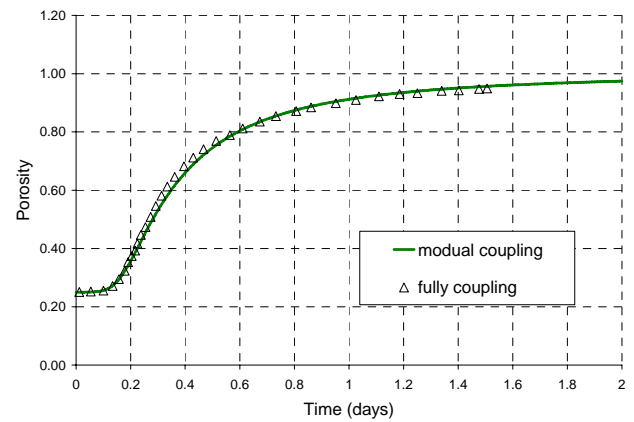


Fig. 4. Porosity history at wellbore.

Three-dimensional computations are conducted using the modular approach subject to one-

dimensional conditions. The results are matched well with original results obtained from one-dimensional fully coupled results [2,3], as shown in Figure 3 and 4.

4. NUMERICAL EXAMPLES

As reported frequently, high water saturation and content significantly increase sanding potential as it destroys the capillary force and may reduce the mechanical strength of formation. Hence, this section examines the capacity of the model with an emphasis on multiphase and 3D effects. Geomechanical aspects were addressed by [8].

4.1. Water-cut effect

In the following simulation, a numerical example of a light oil reservoir in North Sea is examined. This horizontal well lies 2670 meters below surface with a total length of 100 meters. An active aquifer acts at elevation 2672.8 meters. The formation of this reservoir is sandstone with initial oil saturation of 0.8. The initial reservoir pressure is 28MPa with a bubble point pressure at 22.97MPa. The well is operated in first drawdown at 2MPa for 1.03 days and second drawdown at 3MPa for 3.97 days. Drainage influence zone is about 412m in diameter. The three-dimensional analysis over the total well length with various perforation intervals is possible, but is computationally intensive. To simplify this issue, we assume that the horizontal well is uniformly perforated throughout the well, so that much-less-computational cost will be needed when the 3D computation is subject to 2D conditions. The 3D effect with perforations will be examined in later section. Some basic reservoir data and modeling parameters are listed in Table 1.

Table 1 Basic reservoir data and model parameters

| | | |
|----------------------------------|-----------------------------------|----------------------------------|
| $\lambda_0 = 0.5 \text{ m}^{-1}$ | $\rho_s = 2.67 \text{ g/cm}^3$ | $\rho_o = 0.98 \text{ g/cm}^3$ |
| $\rho_w = 1.0 \text{ g/cm}^3$ | $c_o = 5.0\text{E-}06/\text{KPa}$ | $c_w = 4.7\text{E-}7/\text{KPa}$ |
| $K_0 = 0.1 \text{ Darcy}$ | $\mu = 5 \text{ cp}$ | Porosity = 0.17 |

Figure 5 shows the reservoir pressure gradually decline to 25.5Mpa over five days. As production starts, well production is constrained by fluid rate at 100 m³/day for 0.1 day. As the rate declines, bottom hole pressure (BHP) constraint is triggered with a value of 26MPa to stimulate the 2MPa drawdown. After 1.03 days, a sudden jump of oil rate with a value of 42 m³/day is produced since BHP becomes 25MPa as shown in Figure 6. Figure 7 shows the water-cut keep increasing at wellbore over time.

Figure 8 shows high water saturation at wellbore on day five due to water conning.

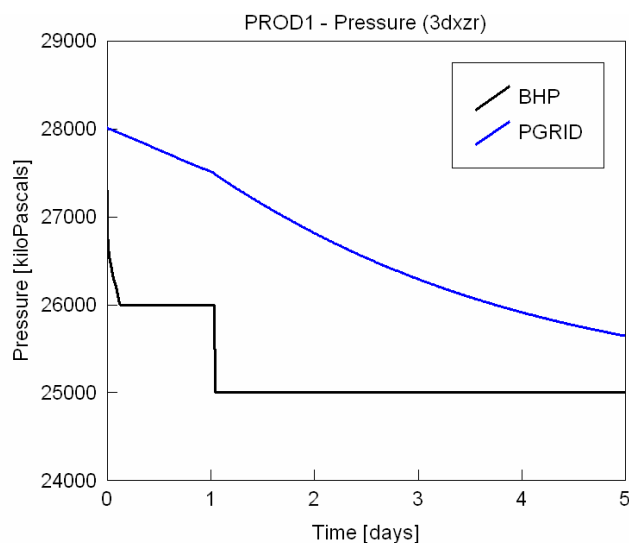


Fig. 5. Reservoir and bottom hole pressure profile over time.

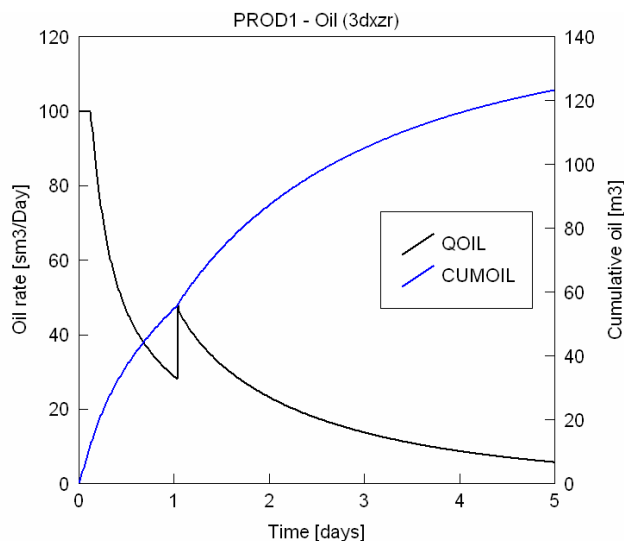


Fig. 6. Oil rate and cumulative oil at wellbore.

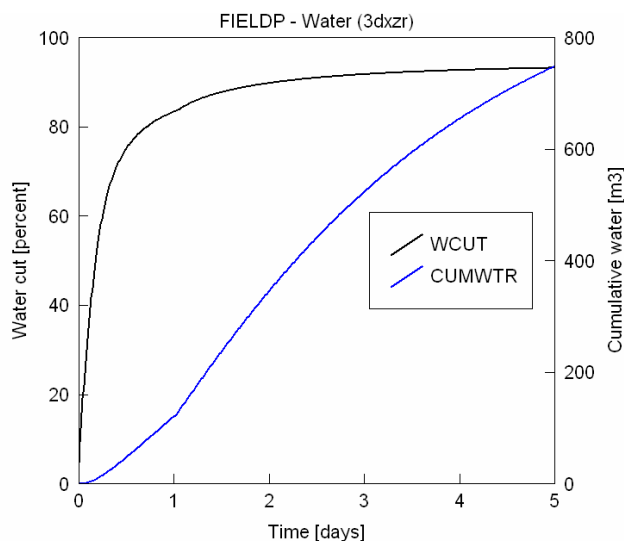


Fig. 7. Water-cut and cumulative water history at wellbore.

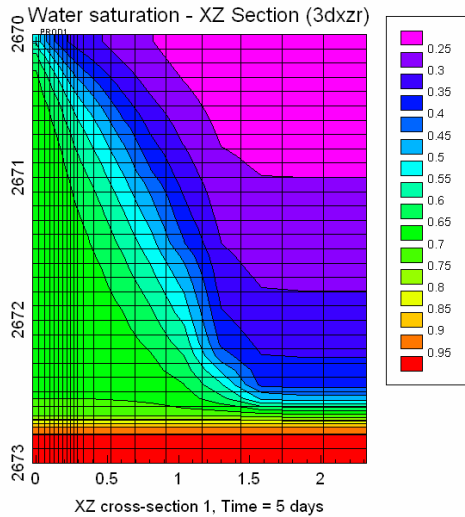


Fig. 8. Water saturation distribution at time = 5 days.

Figure 9 shows the comparison of sand rate with/without water-cut effect. When taking the water-cut effect into consideration, sand rate keeps increasing at 0.2 days when the water-cut reaches a value of 0.6 in Figure 7. Massive sand is produced with the rate peak value of 0.018 m³/day at 0.7 days, then decline to 0.012 m³/day at 1.03 days. As drawdown increases from 2MPa to 3MPa, the sand rates peaks again at a further higher value of 0.019 m³/day, then decreases gradually to a near-constant residual value. This is the same trend as field observation. A total of approximately 137kg of sand is produced, while oil production is 122 m³ over the five days production period.

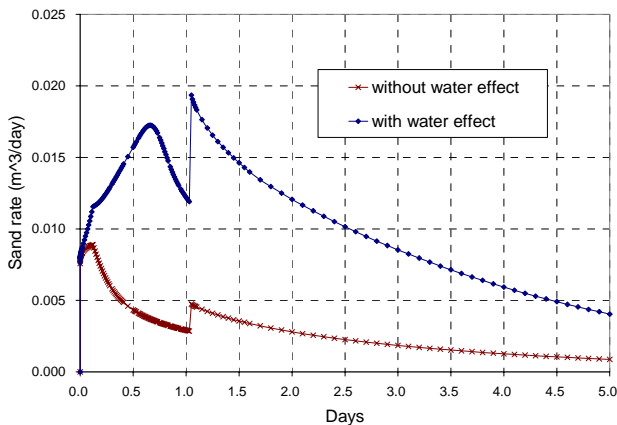


Fig. 9. Sand rate history at wellbore.

On the contrary, oil well will experience much less sand rate, reaching first peak at 0.2 days with a sand rate of 0.08 m³/day, then decline gradually to an almost constant residual value. When the drawdown increases at 1.03 days, sand saturation also peaks, but at a much lower value of 0.05 m³/day, then

follows the declining curve as shown in Figure 9. Correspondingly, the accumulative sand production over the five days is 38 kg, which is 73% less than that with water-cut effect (Figure 10).

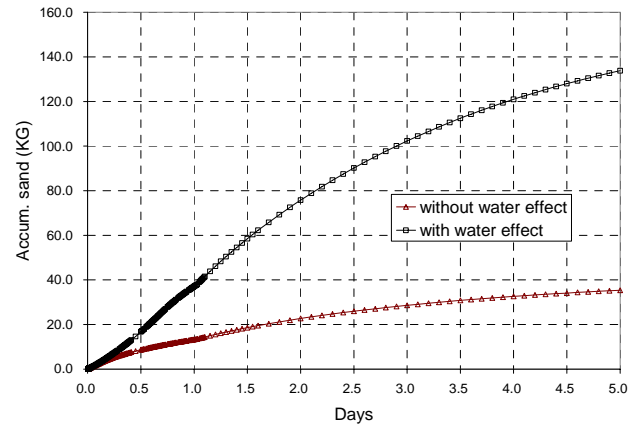


Fig. 10. Accumulated sand history at wellbore.

To summarize, water-cut has significant impact on sand production since it destroys capillary cohesion, resulting in a lower strength of the failed (plastic) zone around the wellbore. Water breakthrough results in a burst of sand production till the cavity is re-stabilized due to sand arching. After each burst, the sand rate decreases gradually to a near-constant residual value. The residual constant sand-rate value appears to grow with increasing drawdown.

4.2. 3D effect

In the following simulation, a vertical offshore well in North Sea is examined by 3D effect (perforations). This well is perforated from 2630m to 2711m with a density of 21 shots per meter. The initial reservoir pressure is 28MPa with a bubble point pressure of 22.97MPa. In order to conduct 3D simulation, a 4-meter thickness layer (z-direction) is chosen from elevation 2670m downwards, where two perforations are chosen within the first two blocks with a grid size (0.1x0.1x0.1m). The permeability in horizontal directions (x- and y-direction) is 0.1 Darcy, while the vertical permeability is 0.1 Darcy for the first 0.5m and 0.01 Darcy for the rest. Drainage influence zone in horizontal directions is 225.6m. Dynamic time step is controlled by reservoir module based on user-defined maximum and/or minimum changes of pressure, saturation, etc., in grid blocks. The simulation is carried out over five days by the same pattern as before: first drawdown at 2MPa for 1.03 days and second drawdown at 3MPa for 3.97 days. The reservoir pressure is slightly declined during the period of simulation time as shown in Figure 11.

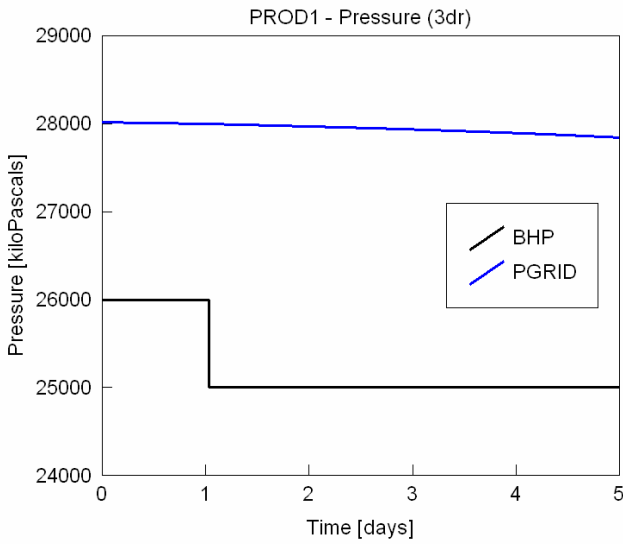


Fig. 11. Reservoir and bottom hole pressure profile over time.

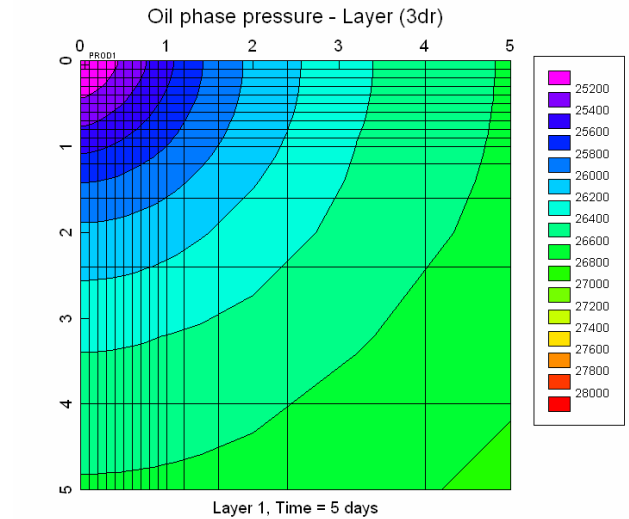


Fig. 13. Horizontal pressure distribution at time = 5 days.

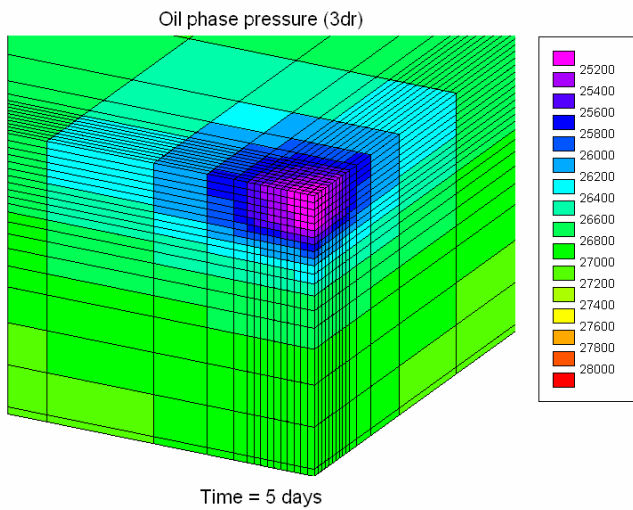


Fig. 12. Pressure distribution at time = 5 days.

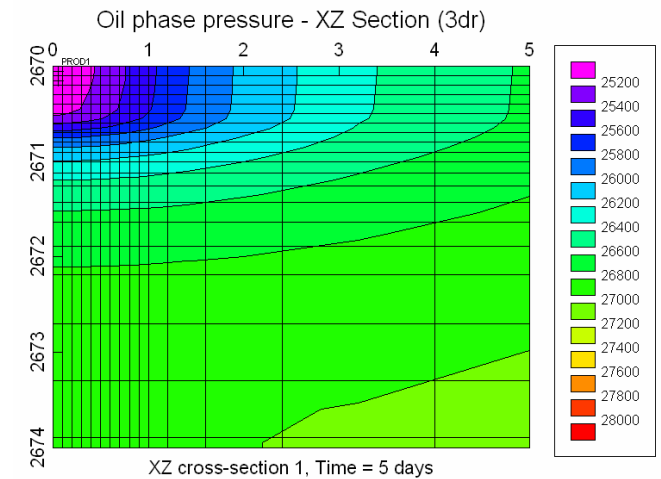


Fig. 14. Vertical pressure distribution (XZ and YZ) at time = 5 days.

Figure 12 shows the three-dimensional pressure distribution on day five. Due to the anisotropic distribution of permeability, the pressure profile has a circular distribution in horizontal direction (x- and y-direction) in Figure 13, while an elliptic distribution in xz and yz section as shown in Figure 14. Figure 15 shows the oil rate and cumulative oil over 5 days at wellbore. During the first drawdown, oil rate declines from the initial 2.2 m³/day to a almost-steady rate 2.01 m³/day due to the initial compressible fluid effect. As sand being produced, permeability increases around wellbore. An increased oil rate is obtained after second drawdown. On day five, an oil rate of 6.2 m³/day is obtained despite the slightly declined reservoir pressure. A total volume of 18 m³ oil is produced over the simulation period.

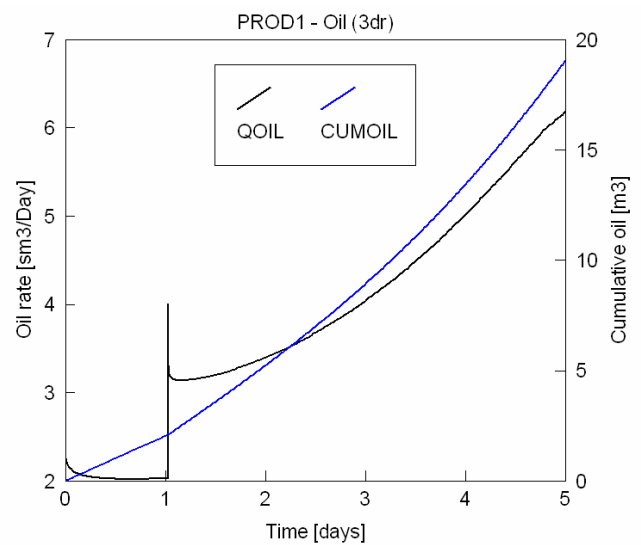


Fig. 15. Oil rate and cumulative oil at wellbore.

Figure 16 shows the porosity profile for the perforation layer over time in horizontal direction.

The porosity increases as solid particles are eroded away, resulting in higher permeability and lower pressure gradient in the erosion zone. Figure 17 shows a 3D close-up of increased porosity distribution around wellbore. Due to anisotropic permeability distribution, an enhanced porosity zone evolves ecliptically as shown in Figure 18-21 for XZ or YZ cross section 1 to 4 on day five. It is noticeable that high porosity zone coincides the pressure distribution.

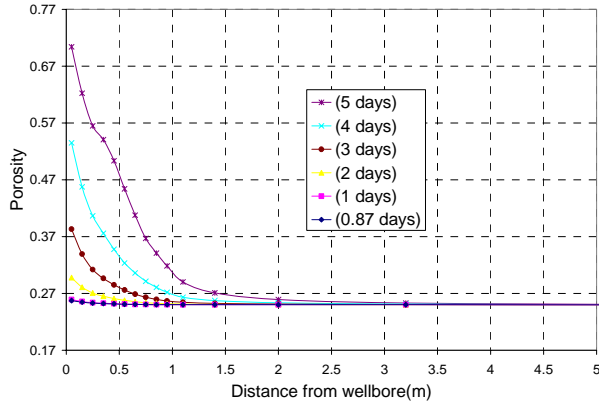


Fig. 16. Porosity profile along horizontal (x or y) direction at different time.

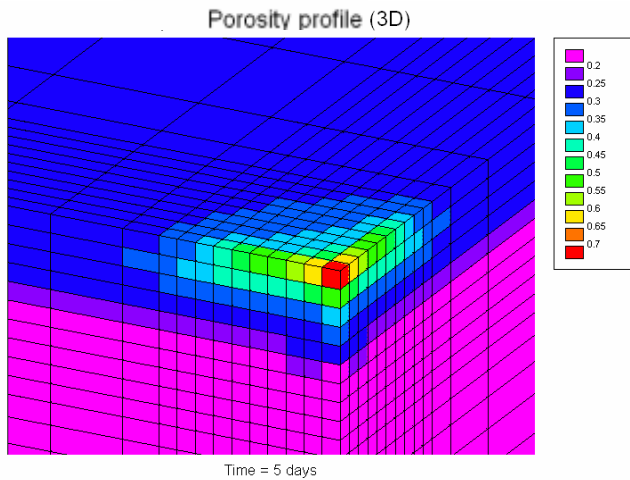


Fig. 17. Three-dimensional porosity distribution at time = 5 days.

As sand particles are eroded, they will be transported to the wellbore where sand is being produced. Figure 22 shows the fluidized sand saturation profile over time for the perforation layer in horizontal directions. A gradual increase of sand saturation to the maximum value of 0.6% at wellbore on day five indicates that this well still has potential to produce sand. The sand rate gradually increase to 0.015 m³/day which is confirmed in the

filed observation with total 101 kg sand being produced (Figure 23).

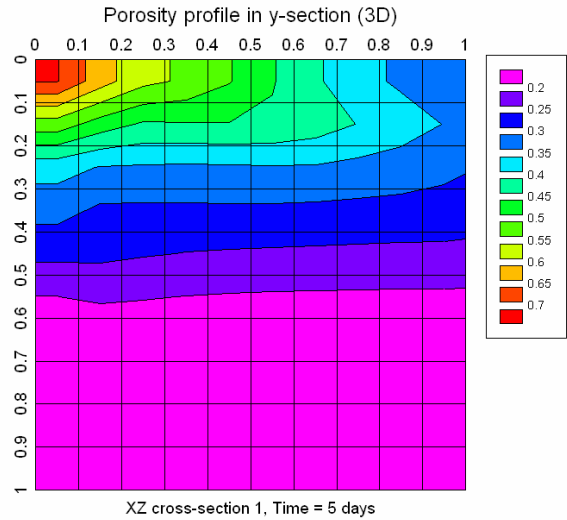


Fig. 18. Porosity profile at XZ cross section 1 (time = 5 days).

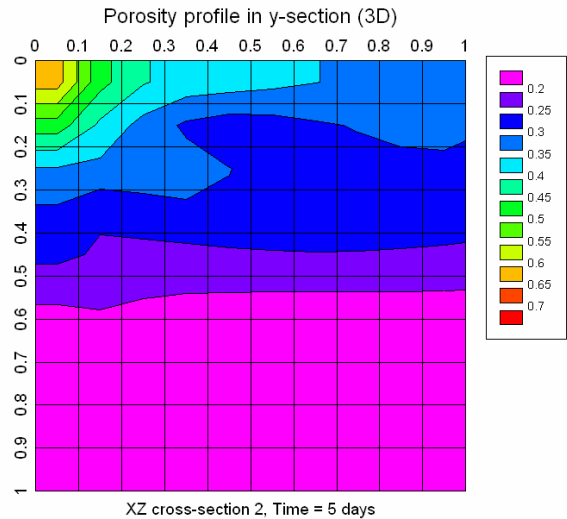


Fig. 19. Porosity profile at XZ cross section 2 (time = 5 days).

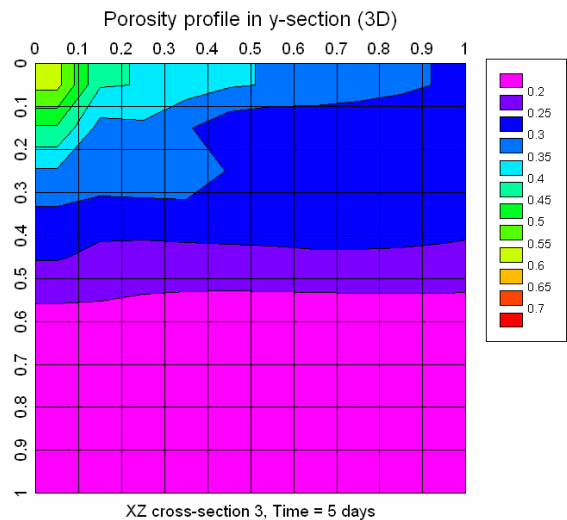


Fig. 20. Porosity profile at XZ cross section 3 (time = 5 days).

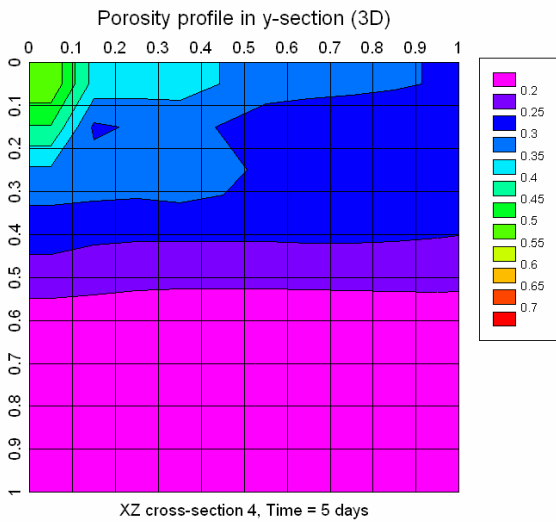


Fig. 21. Porosity profile at XZ cross section 4 (time = 5 days).

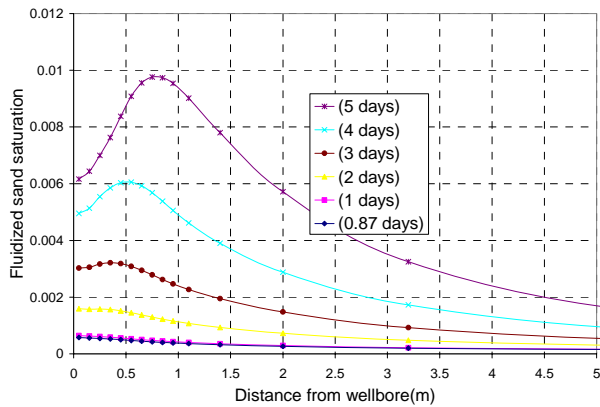


Fig. 22. Fluidized sand saturation profile.

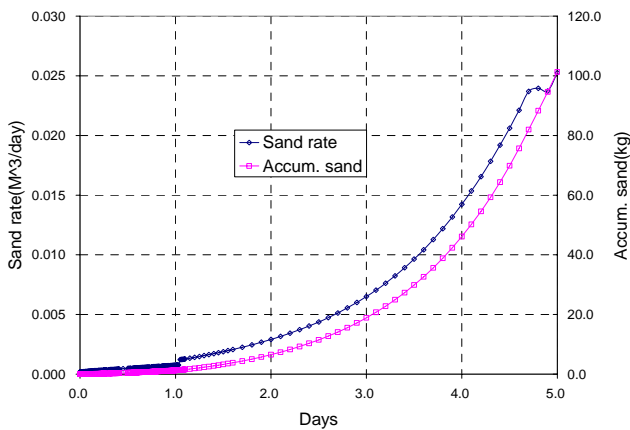


Fig. 23. Accumulated sand and sand rate history at wellbore.

5. CONCLUSIONS

This paper extends earlier work on sand production modeling and presents an integrated modular approach to predict volumetric sand production and cavity growth under three-dimensional, multiphase flow conditions. This model is based on mixture theory with erosion mechanics, in which multiphase

hydrodynamics and geomechanics are coupled in a consistent manner. A modular approach is adopted to effectively take advantage of the current advanced standard reservoir and stress-strain models. The mathematical model is implemented into three integrated computational modules, i.e. erosion module, reservoir module, and geomechanics module. The key idea in the modular system is the reformulation of the stress-flow-erosion coupling so that any existing advanced stress and reservoir code can be incorporated with minimum development effort. The stress, flow and erosion equations are solved separately for each time increment. The coupling terms (porosity, permeability, plastic shear strain, etc.) are passed among them or iterated until convergence is achieved on a time step basis. The system is powerful in terms of its capabilities, yet practical in terms of the computer requirements.

Numerical results show that the water-cut effect is significant and can be captured using the weighting factor to each phase. The weighting factor can be linked to material properties, such as capillary cohesion and rock wetness. It is found that there is an intimate interaction between flow behavior and sand erosion activity. Porosity evolves in time and space as erosion progresses with initial drawdown. In turn the permeability of formations increases due to the porosity changes. This amplifies the erosion activity by virtue of increased flow rate. The self-adjusted mechanism enables the model to predict both the volumetric sand production and the cavity growth based on fluidized sand and porosity profile.

Due to heterogeneity and anisotropy of reservoir formation, the erosion intends to intensify in the higher permeability zone where fluid can easily flow. Resulting cavity grows and propagates in the higher fluid velocity zones. The model can be used for wellbore stability analysis and design in open-hole completions, perforation pattern design, as well as volumetric sand prediction with different pumping strategies to optimize of the hydrocarbon production.

6. ACKNOWLEDGEMENTS

The authors wish to express their sincere gratitude for funding provided by Alberta Ingenuity Fund (AIF) and financial support from Halliburton Energy.

REFERENCES

1. Wang, J. 2003. Mathematical and numerical modeling of sand production as a coupled geomechanics-hydrodynamics problem. Calgary. (PH. D. dissertation)
2. Vardoulakis, M. Stavropoulou and P. Papanastasiou. 1996. Hydromechanical aspects of the sand production problem. *Transport in Porous Media*. 22, 225-244.
3. Wan, R.G. and J. Wang. 2002. Modelling sand production within a continuum mechanics framework. *Journal of Canadian Petroleum Technology*. 41:4, 46–52.
4. Wan, R. G. and J. Wang. 2003. Modeling sand production and erosion growth under combined axial and radial flow. *SPE International Thermal Operations and Heavy Oil Symposium and International Horizontal Well Technology Conference* SPE 80139. Calgary, Canada, 4–7 November 2002.
5. Wang, J. and R.G. Wan. 2004. Computation of sand fluidization phenomena using stabilized finite elements, *Finite Elements in Analysis and Design* 40:1681-1699.
6. Wang, J., R. Wan, A. Settari, D. Walters, and Y. N. Liu, Sand production and instability analysis in a wellbore using a fully coupled reservoir-geomechanics model, Gulf Rocks 2004, *the 6th North America Rock Mechanics Symposium (NARMS): Rock Mechanics Across Borders and Disciplines*, held in Houston, Texas, June 5 – 9, 2004.
7. Wan, R.G. and J. Wang 2004. Numerical modeling of sand production in an oil well of the Messla field. Research Report Submitted to Golder Associates, 36p.
8. Wang, J., R. Wan, A. Settari, D. Walters. 2005. Prediction of volumetric sand production and wellbore stability analysis of a well at different completion schemes. Alaska Rocks 2005, *the 40th U.S. Symposium on Rock Mechanics (USRMS): Rock Mechanics for Energy, Mineral and Infrastructure Development in the Northern Regions*, held in Anchorage, Alaska, June 25-29, 2005.
9. M. Stavropoulou, P. Papanastasiou and I. Vardoulakis. 1998. Coupled wellbore erosion and stability analysis. *Int. J. Numer. Anal. Methods Geomech.* 22, 749-769
10. Hughes, T.J.R., L.P. Franca, and G.M. Hulbert. 1989. A new finite element formulation for computational fluid dynamics, The Galerkin/least-squares method for advective-diffusive equations. *Comput. Methods Appl. Mech. Engrg* 73, 173-189.
11. Aziz, K, and A. Settari. 1979. *Petroleum reservoir simulation*. London. Elsevier Applied Sci.
12. Settari, A. and D. A. Walters. 2001. Advances in coupled geomechanical and reservoir modeling with applications to reservoir compaction. *SPE Journal*. 9: 334–342.